Archives of Biochemistry and Biophysics 762 (2024) 110212

Contents lists available at ScienceDirect

Archives of Biochemistry and Biophysics

journal homepage: www.elsevier.com/locate/yabbi

Purification and catalysis of choline dehydrogenase from *Escherichia coli*

Xiuxiu Ma [a,1], Fangling Xu [a,1], Koukou Yu [a], Fan Wang [a], Quan Li [a], Weifeng Liang [a], Bing Liu [a], Bo Zhang [b], Jiapeng Zhu [a,c,d,**], Jiao Li [a,c,d,e,*]

[a] School of Medicine, Nanjing University of Chinese Medicine, 210023, Nanjing, China
[b] School of Life Sciences, Nanjing University, 210023, Nanjing, China
[c] Jiangsu Key Laboratory for Pharmacology and Safety Evaluation of Chinese Materia Medica, School of Pharmacy, Nanjing University of Chinese Medicine, 210023, Nanjing, Jiangsu, China
[d] Jiangsu Joint International Research Laboratory of Chinese Medicine and Regenerative Medicine, Nanjing University of Chinese Medicine, 210023, Nanjing, Jiangsu, China
[e] Key Laboratory of Drug Target Research and Drug Discovery of Neurodegenerative Disease, Nanjing University of Chinese Medicine, 210023, Nanjing, Jiangsu, China

A B S T R A C T

Choline dehydrogenase (CHDH) is a membrane-bound enzyme belonging to the glucose-methanol-choline (GMC) oxidoreductase superfamily, which is characterized by a crucial FAD-binding domain essential for catalytic function. CHDH catalyzes the oxidation of choline to betaine aldehyde, which is further oxidized to betaine, a vital osmoprotectant and methyl donor for cellular physiology and metabolism. However, the detailed catalytic mechanism of CHDH still remains poorly understood. In our investigation, we gained purity *E. coli* CHDH samples in DDM (n-dodecyl-β-D-maltoside) and SMA (styrene maleic acid) copolymer respectively and examined their structural composition and catalytic activity separately. Our findings demonstrated the effectiveness of SMA, commonly employed for extracting transmembrane proteins and can preserve the natural bio-membrane environment surrounding the enzyme, in extracting peripheral membrane proteins like CHDH here, which lacks transmembrane helices. CHDH exhibited a trimeric conformation in SMA, whereas it existed as monomers in DDM, as determined by our negative staining analysis. Our experiments also revealed that highly pure *E. coli* CHDH could only oxidize choline to betaine aldehyde but failed to further oxidize betaine aldehyde to betaine as determined by the biochemical and enzymatic reaction kinetic assays. In addition, the enzyme in SMA displayed greater catalytic activity compared to that in DDM. Furthermore, we confirmed the crucial role of His473, which is hypothesized to be a critical site for substrate binding from our structural comparative analysis between CHDH and its highly homologous choline oxidase, in the catalytic activity of the enzyme through gene mutation. Our work also sheds light on CHDH's contribution to cellular osmotic tolerance through gene knockout. This research enhances our better understanding of CHDH within cellular biochemistry and metabolic pathways.

1. Introduction

Choline dehydrogenase (CHDH), initially characterized by Mann and Quastel in 1937 [1], is primarily located in the cell membrane of prokaryotes and the inner mitochondrial membrane of eukaryotes, playing a crucial role in electron transfer processes within the respiratory chain [2–4]. As previously reported, CHDH catalyzes the oxidation of choline to betaine, one of the limited osmoprotectants utilized by cells to compensate for the impacts of high osmotic stress, such as high salt, freezing temperatures, and extreme heat. An intermediate product in the overall choline oxidation process is betaine aldehyde [2,5,6].

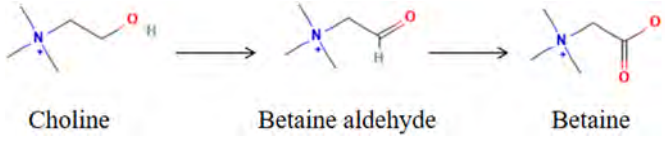

* Corresponding author. School of Medicine, Nanjing University of Chinese Medicine, Nanjing, 210023, China.
** Corresponding author. School of Medicine, Nanjing University of Chinese Medicine, Nanjing, 210023, China.
E-mail addresses: zhujiapeng@hotmail.com (J. Zhu), jiao.li@njucm.edu.cn (J. Li).
[1] These authors contributed equally to this work.

https://doi.org/10.1016/j.abb.2024.110212
Received 5 August 2024; Received in revised form 3 November 2024; Accepted 4 November 2024
Available online 5 November 2024

For microorganisms, the accumulation of betaine in the cytoplasm is crucial for controlling intracellular water content by regulating the levels of intracellular solutes [7]. In a high-saline environment, the failure to do so can lead to consequences like dehydration, osmotic shock, and plasmolysis. Several human pathogens, including *Escherichia coli*, *Staphylococcus aureus*, *Pseudomonas aeruginosa*, *Enterococcus faecalis*, *Klebsiella pneumoniae*, and *Vibrio parahaemolyticus*, rely on the accumulation of betaine to adapt to the high osmotic conditions encountered at sites of human infection [8].

In humans, CHDH is associated with various pathologies, including male infertility, homocystinuria, metabolic syndrome, high risk of cardiovascular diseases, and breast cancer. Its crucial role in metabolism and oxidative stress is highlighted, and the need for comprehensive research into its molecular mechanisms is of massive importance. Moreover, betaine, the final oxidation product of choline, serves as an important osmoprotectant in the kidney and also acts as a methyl donor in the biosynthesis of methionine. These functions underscore the significance of betaine biosynthesis as a noteworthy target for metabolic engineering [9,10].

As established by previous research, CHDH belongs to the glucose-methanol-choline (GMC) enzyme oxidoreductase superfamily based on its structural arrangement [9,11,12]. This superfamily comprises a group of oxidoreductases that share a common structural fold, with FAD serving as a coenzyme that primarily catalyzes the oxidation of alcohol groups into their corresponding aldehydes [13]. Enzymes within this family feature a 30-amino acid region near the amino terminus, corresponding to the ADP-binding domain of FAD, and a steroid-binding domain in the C-terminal region [14–16]. Despite the substantial interest in CHDH, its biochemical characterization has lagged behind its medical and biotechnological applications due to the enzyme's high instability when removed from the membrane and the challenges associated with obtaining high yields and purity of the enzyme sample in eukaryotic cells. The highly purified preparation is required to obtain stable CHDH—a goal that poses a big challenge, all the characteristics of CHDH reported so far were obtained using relatively crude preparations, and highly purified preparations are imperative in the field [17]. This challenge has led to limited or potentially misleading structure-function studies, leaving much unknown about the biochemical features of CHDH.

A previous study has reported that *E. coli* CHDH can oxidize choline to produce betaine aldehyde and then oxidize betaine aldehyde to produce betaine at a similar rate [4]. Alternatively, some other studies have suggested a two-step process, with the initial step involving the oxidation of choline to betaine aldehyde by CHDH encoded by the *betA* gene, and the subsequent step involving further oxidation of betaine aldehyde to betaine, carried out by the betaine aldehyde dehydrogenase encoded by the *betB* gene in *Staphylococcus aureus* [18]. However, these previous studies both had faced challenges related to sample purification, which contained impurities that could introduce interference in the experimental results to some extent.

DDM was considered the most traditional and classic detergent, making it the top choice for extracting membrane proteins [19]. The method effectively isolated membrane proteins by creating lipid-detergent mixed micelles that replaced the native membranes around them. For some membrane proteins in DDM, their stabilities are relatively low as the micelles cannot preserve the native conformation of the protein [20,21]. This limitation hinders both structural and functional investigations of membrane proteins, as well as their subsequent applications. In contrast, SMA offers a significant advantage over traditional detergents by enabling the extraction of the target protein along with the natural lipid bilayer and associated proteins through the spontaneous formation of SMA lipid particles (SMALPs) [22]. In addition, SMALPs exhibit remarkable stability during the purification process [23].

Here, we purified *E. coli* CHDH using SMA3000 and DDM respectively to obtain high-purity enzyme, facilitating a comprehensive evaluation of its structural, biochemical, and characteristics. The results of this research will deepen our understanding of the basic biological mechanisms underlying *E. coli* CHDH catalysis and provide a valuable model for studying similar enzymes in eukaryotes.

2. Results

2.1. The purification and composite analysis of CHDH

To provide insight into the enzymatic activity of CHDH, we employed both the SMA3000 copolymer to extract small lipid bilayer discs encapsulated within the polymer, referred to as SMALPs (SMA lipid particles) and the commonly used detergent DDM to isolate the membrane-bound enzyme for sample purification. The size of the enzyme in SMA3000 was bigger than that by DDM from FPLC SEC chromatogram curves (Fig. 1A). The purified samples were identified by SDS-PAGE (Fig. 1B), and it was clear that the purity of the samples was very high in our research. To deeper into their structural composite, these samples were examined using negative staining electron microscopy (EM). It revealed significant size discrepancies between the enzyme particles in SMA3000 and DDM, characterizing trimer in SMA3000 and monomer in DDM, which was consistent with the FPLC SEC chromatogram results (Fig. 1C and **D**).

Subsequently, a set of negative staining EM data was collected for *E. coli* CHDH in SMA3000 for further investigation. The original raw micrographs were used for particle picking and selection. The 2D classification images confirmed the assembly of the sample purified by SMA3000 as a clover-shaped trimer. A 3D map was constructed using CryoSPARC v3.2 (Fig. 1E). Then we used the Alphafold2 model for trimeric CHDH (Fig. 1F) to fit in the map, and most regions of the map were well fitted (Fig. 1E), which indicated that the predicted trimeric model for CHDH was plausible.

Additionally, we conducted cryo-EM structural research using the purified sample of CHDH in SMA3000. We observed that the trimeric configuration tended to dissociate into monomers after cryogenic processing, and the particles showed inhomogeneity from our electron microscopy images. Due to the small size of the CHDH monomer particles and the challenges posed by their orientation advantages, our attempts to obtain a cryo-EM 3D map of the monomer were unsuccessful.

2.2. The catalytic process of E. coli CHDH

As shown in Fig. 2A, the standard sample of betaine aldehyde was baseline resolved by HPLC, with a peak at 5 min retention time. Owing to the impurities contained in the commercial betaine aldehyde, an interfering peak emerged at 1.7 min, but the main and interference peaks were completely separated. When using PMS or decylubiquinone (DQ) as electron acceptors, *E. coli* CHDH effectively oxidized choline and yielded products with a matching 5 min peak of standard betaine aldehyde (Fig. 2B and C). In contrast, there was no such peak in the blank group when using ddH_2O as an electron acceptor (Fig. 2D). Therefore, *E. coli* CHDH can oxidize choline to betaine aldehyde.

To determine whether the enzyme has the function to further oxidize betaine aldehyde to betaine, the standard sample of betaine was baseline resolved with peaks at 5.1 min, 6.3 min, 7.1 min, and 8.3 min as shown in Fig. 2E. In the reaction groups using betaine aldehyde as substrate, and PMS and DQ as electron acceptors, only a single peak at 8.3 min was observed (Fig. 2 F, G, and H). There was the same 8.3 min peak that appeared in the blank group when using ddH_2O as an electron acceptor (Fig. 2H). Then mass spectrometry analysis confirmed that the peak at 8.3 min corresponded to betaine aldehyde and the peak at 6.3 min corresponded to betaine, indicating that *E. coli* CHDH lacks the catalytic function to further oxidize betaine aldehyde to betaine.

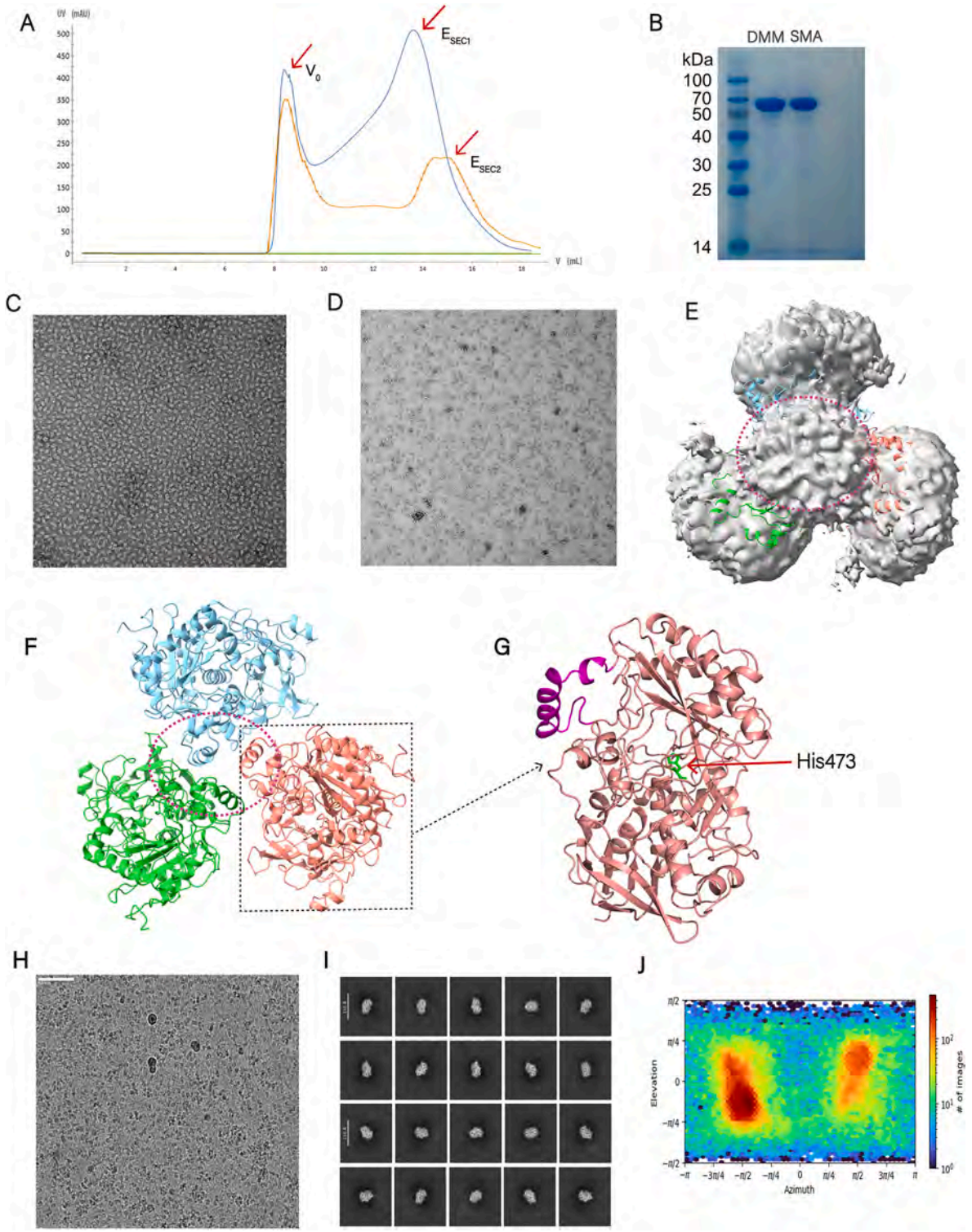

Fig. 1. The purification and model of *E. coli* CHDH. (A) FPLC SEC chromatograms of CHDH in SMA and DDM copolymers on a Superose 12 10/300 GL column. The FPLC SEC chromatogram of CHDH in the SMA3000 copolymer displayed a sharp peak at 13.5 mL, about 180 kDa (E_{SEC1}), while the chromatogram of CHDH in the DDM copolymer displayed a sharp peak at 15 mL, about 60 kDa (E_{SEC2}), with the curves colored in blue and orange, respectively. V_0, the void volume of the column. **(B)** Coomassie blue stained SDS-PAGE gel showed one band between 50 kDa and 70 kDa for CHDH samples in DDM and SMA3000, respectively. The negative staining particles of CHDH in SMA3000 (**C**) and DDM (**D**) were obtained by Talos™ L120C TEM. Both magnifications are 57,000. **(E)** The negative staining 3D construction map for CHDH in SMA3000 copolymer fitted with the top Alphafold2 Multimer output model (high confidence score reaches to 98). The middle junctional region, possibly the membrane-bound region, was outlined by magenta dashed ellipse. **(F)** The output model of Alphafold2 Multimer on COSMIC[2] of the trimeric CHDH. The middle junctional region was outlined as shown in **E**. **(G)** One monomer of the trimeric CHDH. The residue of His473 was highlighted in the stick in red. The possible regions of membrane-bound and nucleotide binding were colored in magenta and cyan, respectively. **(H)** Representative cryo-EM micrograph of *E. coli* CHDH. The scale bar is 50 nm. **(I)** Class averages after the final round of two-dimensional classification, were sorted in descending order by the number of particles in each class. **(J)** Gold standard FSC curve from cryoSPARC and orientation plot of particles included in the final 3D reconstruction for CHDH monomer.

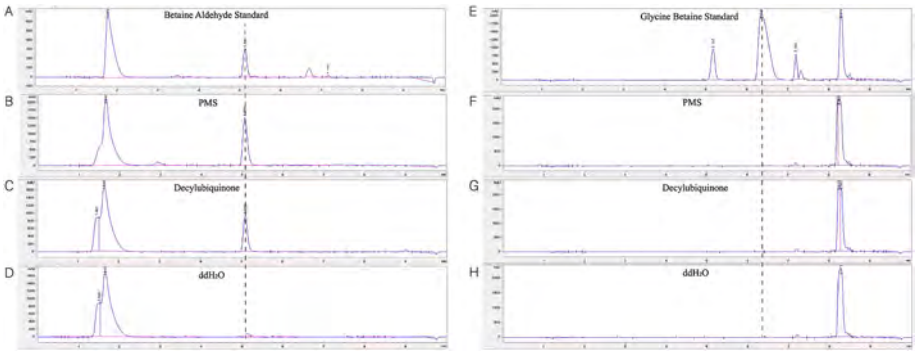

Fig. 2. HPLC chromatogram of standard samples and the products of CHDH-catalyzed reactions. (A) The HPLC chromatogram of standard betaine aldehyde. HPLC chromatograms of products of CHDH-catalyzed reactions using choline as substrate, and PMS **(B)**, DQ **(C)**, and ddH_2O **(D)** as electron acceptors, respectively. **(E)** The HPLC chromatogram of standard betaine. HPLC chromatograms of products of CHDH-catalyzed reactions using betaine aldehyde as substrate, and PMS **(F)**, DQ **(G)**, and ddH_2O **(H)** as electron acceptors, respectively.

2.3. The comparison of E. coli CHDH and choline oxidase and the significance of His473 in E. coli CHDH

Aligning the amino acid sequences of *E. coli* CHDH and choline oxidase (Fig. 3A), and comparing the predicted model of *E. coli* CHDH with the crystal monomer structure of choline oxidase (Fig. 3D), they revealed high similarities between the two enzymes, particularly in the FAD and substrate binding domains (Fig. 3E). Upon examining the crystal structure of choline oxidase complexed with betaine (PDB 4MJW) [18], we confirmed that the carboxylate of betaine closely interacts with the flavin (Fig. 3B and C), and additional interactions involve the carboxylate group with the protein through the side chains of H466 and N510 (Fig. 3E), which locate at the same positions of H473 and N515 in CHDH. Additionally, the region 250–255 in choline oxidase presents a flexible loop (depicted in red cartoon in Fig. 3B and **C**), which plays a crucial role in the enzyme's catalytic process. In contrast, this region in CHDH is a helix, supposed to constitute a membrane contact surface based on our negative staining map (Figs. 1E, 1G and 3D). This may lead to differences in assembly modes between the two enzymes, with choline oxidase forming a dimer and CHDH forming a trimer. Despite their similar monomeric structures, their catalytic mechanisms differ.

H473 in CHDH is positioned similarly to H466 in choline oxidase, where H466 interacts with the substrate and plays an important role in the catalytic process of choline oxidase. Therefore, we hypothesized that H473 may perform a similar role in CHDH. To validate this hypothesis, a mutant CHDH with H473 replaced by alanine was investigated. It can be seen from the FPLC SE chromatographic curve of the $CHDH_{H473A}$ (Fig. 3F) was similar to that of wild-type CHDH (Fig. 1A), representing that the $CHDH_{H473A}$ is correctly folded. Notably, the $CHDH_{H473A}$ variant exhibited no detectable oxidation activity towards choline in *vitro* (compared to Fig. 3 G and **H**), providing strong evidence for the critical catalytic role of H473 in the catalytic activity of CHDH.

2.4. Comparison of the catalytic activity of E. coli CHDH in DDM and SMA3000

The CHDH samples purified by SMA3000 and DDM, respectively, were employed for the detection of enzyme activity. When using PMS as the electron acceptor, the K_m values for CHDH purified by SMA3000 and DDM were 9.00 mM and 9.86 mM. The k_{cat} values were 50.90 s^{-1} and 9.70 s^{-1} (Fig. 4 A and **B** and Table 1). It revealed that the K_m values for CHDH purified by SMA3000 and DDM were similar, but the k_{cat} and k_{cat}/K_m values for the enzyme in SMA3000 were approximately five times higher than that in DDM. This suggested that CHDH purified by SMA3000 displayed enhanced catalytic efficiency compared with DDM.

As the result shown in Fig. 4 A and **C**, the enzymatic activities of CHDH purified by SMA3000 were detected using PMS or DQ as electron acceptors. When using PMS and DQ as electron acceptors, the K_m values were 9.00 mM and 2.30 mM, the V_{max} values were 34.62 μM/s and 8.60 μM/s, and the k_{cat} values were 50.90 s^{-1} and 12.60 s^{-1}, respectively (Table 1). This suggested that the enzyme of CHDH has a stronger affinity for DQ than for PMS.

2.5. Osmotic stress tolerance mediated by CHDH through the choline-betaine pathway

To assess the contribution of CHDH's oxidative function on osmotic stress tolerance, we conducted a comparative analysis of the growth of wild-type (WT) *E. coli* C43 cell and C43ΔbetA cell in hypersaline conditions and the presence or absence of choline or betaine. As shown in Fig. 5, growth curves of WT *E. coli* C43 cells were consistent in the conditions of the presence of either choline or betaine and higher than those in the presence of high salt alone. The result indicated that choline and betaine could enhance osmotic stress tolerance in *E. coli*, which encoded the *betA* gene and can generate the enzyme CHDH. Conversely, the growth of C43ΔbetA cells had reduced when grown in hypersaline media alone or with the addition of choline but displayed substantial growth improvement when grown in the presence of betaine. We found that choline alone was unable to enhance osmotic stress tolerance without the oxidative function of CHDH in *E. coli*. In contrast, the presence of betaine significantly recovered the growth of C43ΔbetA cells, highlighting the vital role of betaine played in *E. coli*'s resistance to osmotic stress. Thus, our observations suggested that CHDH played a critical role in *E. coli* in response to osmotic stress by mediating the choline-betaine pathway.

3. Discussion

CHDH plays a crucial role in the metabolism and oxidative stress of pathogenic microorganisms and humans. However, the incapability of obtaining high-purity and active samples in previous studies [17], the catalytic characteristics of this enzyme were still not fully understood. Here it is particularly important to conduct fundamental research on the CHDH from *E. coli*, which can be overexpressed in large quantities. This study successfully purified high-purity CHDH using SMA3000 and DDM, marking a significant milestone in the foundational research of CHDH.

At present, the structural information of CHDH is little known in the field, which is of great significance for the understanding of its catalytic mechanism. This research investigates the composition of *E. coli* CHDH and its potential structural model through structural biology methods, confirming for the first time that *E. coli* CHDH exists as a trimer in a natural membrane environment [24]. Based on this important finding, a trimer structural model is constructed for *E. coli* CHDH by combining the

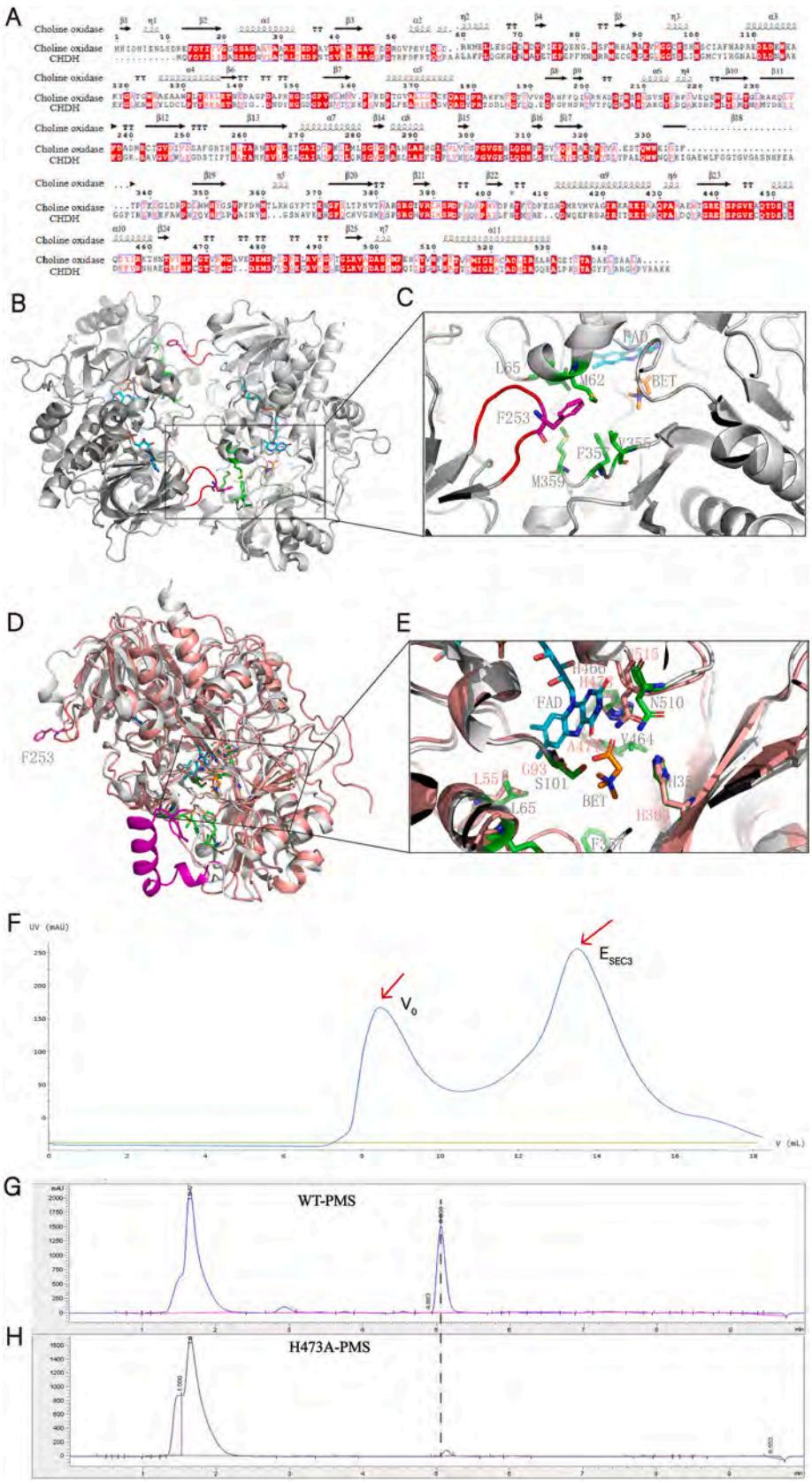

(caption on next page)

Fig. 3. The substrate binding site for CHDH, based on the structure of choline oxidase in complex with betaine. (A) The amino acid sequence alignment of choline oxidase and CHDH. **(B)** The crystallographic homodimeric structure of choline oxidase in complex with the reaction product betaine (PDB entry 4MJW) [18]. Symmetrical active sites were depicted in sticks. **(C)** The magnification of one of the substrate binding sites from **A**. FAD and betaine were shown in cyan and orange sticks, respectively, and the interaction residues in green sticks. The flexible loop 250–255 was shown in the red cartoon, and the F253 residue in this loop was shown in the magenta stick. **(D)** The alignment of the monomer structure of choline oxidase in complex with betaine and the monomer predicted structure of CHDH. The potential membrane-bound region was colored in magenta. The amino acids in CHDH were shown in pink sticks and labeled in pink, meanwhile, the amino acids in choline oxidase were shown in green sticks and labeled in gray. FAD and betaine in choline oxidase were shown in cyan and orange sticks, respectively, along with gray labels. **(E)** The magnification of interaction residues in the active site form **C**. FAD, betaine, and active residues in choline oxidase and the predicted CHDH were shown in the same colors as in **C**. **(F)** The FPLC SEC chromatograms of $CHDH_{H473A}$ in SMA copolymers on a Superose 12 10/300 GL column. The FPLC SEC chromatogram of $CHDH_{H473A}$ in the SMA3000 copolymer displayed a sharp peak at 13.5 mL, about 180 kDa (E_{SEC3}). V_0, the void volume of the column. The HPLC chromatograms of products from the catalyzed reactions of CHDH **(G)** and $CHDH_{H473A}$ **(H)**, both utilized choline as the substrate and PMS as the electron acceptor.

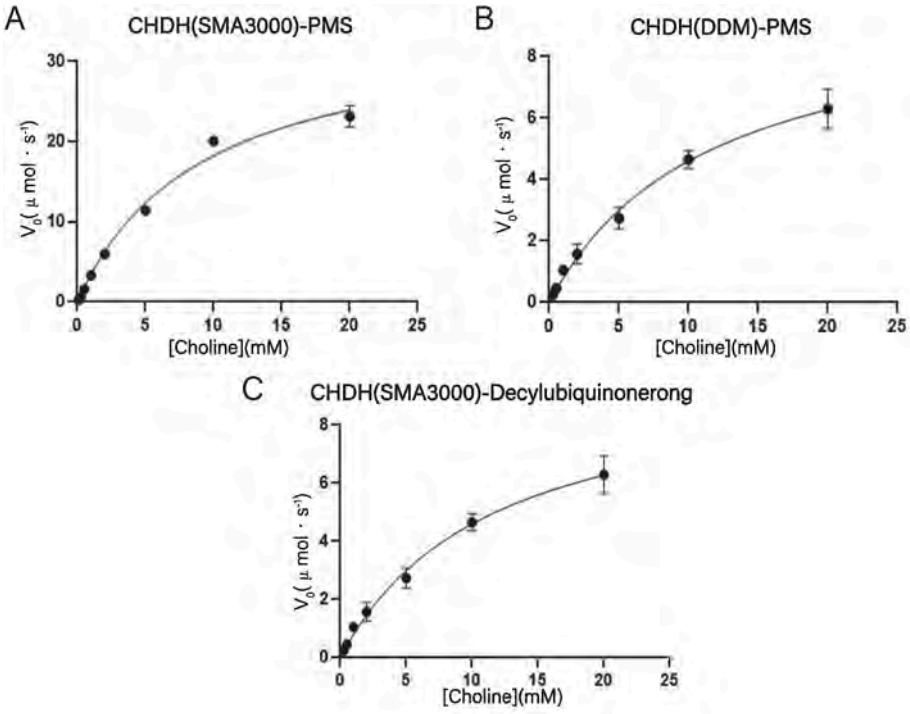

Fig. 4. Steady-state kinetics of CHDH. In all reactions, the substrate employed was choline. All kinetic parameters data were obtained from at least three repeated experiments and are expressed as the Mean ± SEM (standard error of the mean). **(A)** The enzymatic reactions of CHDH, when purified by SMA3000 and using PMS as the electron acceptor, were depicted. **(B)** The enzymatic reaction of CHDH when purified by DDM and using PMS as the electron acceptor. **(C)** The enzymatic reactions of CHDH, when purified by SMA3000 and using DQ as the electron acceptor, were depicted.

Table 1
Kinetic parameters of CHDHs in SMA and DDM, respectively.

Enzyme	Electron acceptor							
	PMS				DQ			
	K_m	V_{max}[a]	k_{cat}[a]	k_{cat}/K_m[a]	K_m	V_{max}	k_{cat}	k_{cat}/K_m
CHDH(SMA)	9.00 ± 0.49	34.62 ± 1.14	50.90 ± 1.67	5.66 ± 0.13	2.30 ± 0.13	8.60 ± 0.21	12.60 ± 0.31	5.48 ± 0.22
CHDH(DDM)	9.86 ± 0.55	11.44 ± 0.66	9.70 ± 0.56	0.98 ± 0.03	–	–	–	–

[a] $p \leq 0.05$.

3D map, generated from the negative staining EM analysis in our work, and the result of Alphafold2 multimeric prediction. Although AlphaFold can predict structures, especially for single-subunit structures, with very high scores, there is still a long way to go in the assembly modes of multimer structures, especially under the condition of without the knowledge of the composite of the enzyme. The high resolution of the structure of CHDH is still necessary for fully understanding the catalytic mechanism of CHDH. We strongly suspect that the junctional region of the trimeric complex is a bio-membrane binding area, and it may be easily destroyed to some extent during the conventional detergent purification process, like DDM, which forms artificial micelles and replaces the native membrane surrounding the enzyme, and thus reducing the enzyme activity as confirmed by our comparative activity studies of *E. coli* CHDH in SMA and DDM.

Despite gaining preliminary insights into the composition of *E. coli* CHDH, the mechanisms by which substrates access the active site and its catalytic mechanisms remain unclear. Notably, choline oxidase, another enzyme involved in the biosynthesis of betaine from choline, has been extensively characterized regarding its mechanistic and structural properties [25–29]. Through comparative analysis, we observed a high degree of sequence and functional similarity between choline oxidase and CHDH enzymes. We proposed the positively charged imidazolium of

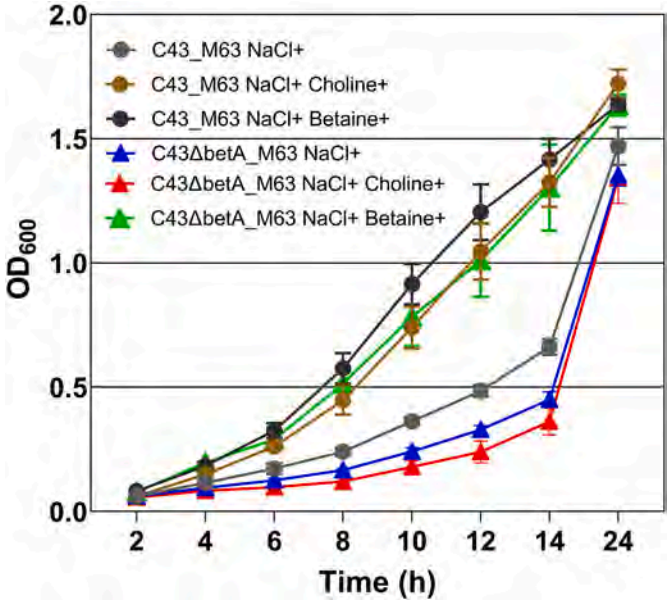

Fig. 5. Effects of deletion of CHDH gene on osmotic stress tolerance of *E. coli* C43 cell. The comparison of growth curves of *E. coli* C43 and C43ΔbetA strains. Growth curves of *E. coli* C43 strains as optical density (OD600) plots, grown in the medias containing 600 mM NaCl, 600 mM NaCl in the presence of either choline or betaine, respectively.

His473 stabilizing the alkoxide reaction intermediate–validated by mutagenesis of H473 to alanine resulting in loss of oxidation activity towards choline in *vitro* [29]. Choline oxidase differs from CHDH only in a loop at the dimer interface (250–255) [29]. This loop's distinct conformations are assumed to regulate substrate access to the active site, by defining varying accessibilities of the proposed entrance. Intriguingly, in CHDH, the corresponding loop region is occupied by an alpha helix as a membrane touch surface. (shown in the magenta cartoon in Figs. 1G and 3D). This alpha helix partially covered the substrate-binding site of CHDH. This structural disparity stands as a key difference between the two enzymes. It is noteworthy to consider that CHDH lacks the capability to further oxidize betaine aldehyde to betaine, the presence of this alpha helix is at least one of the factors, which is also a possible membrane-binding region for its role as a membrane-bound enzyme.

E. coli CHDH is capable of oxidizing choline to betaine aldehyde but cannot further oxidize betaine aldehyde to betaine in our research, which is consistent with the activity of human CHDH, converted choline to betaine aldehyde as reported in previous research [9,30]. However, it contradicts earlier findings that *E. coli* CHDH can oxidize choline to betaine aldehyde and then oxidize betaine aldehyde to betaine at the same rate [4], and here we suspect that the purity of the sample may be the cause of this contradiction. In addition, the enzyme exhibited enhanced efficiency when using PMS as an electron acceptor, but displayed slightly higher affinity when using DQ, a synthetic analogue of coenzyme Q (CoQ, ubiquinone), which is reported as an in *vivo* main electron acceptor for rat liver CHDH in previous research [29,30].

Previous studies have reported that betaine has adaptive effects under high salt osmotic stress, however, there have been no reports on whether it serves a similar function in pathogenic microorganisms like *E. coli*, nor on the potential role of CHDH in this process. In our work, the C43ΔbetA strain, which cannot synthesize CHDH, showed a deficiency in choline dehydrogenase activity. It failed to utilize choline but continued to use betaine as an osmoprotectant to support growth. Choline and betaine aldehyde served as precursors in osmotically stressed cells. Elevated external osmotic pressure prompted the activation of transport systems, facilitating the influx of choline in WT *E. coli* [31]. This influx, in turn, stimulated the initiation of the choline-betaine pathway, with CHDH playing a crucial role in the initial oxidation step. It shed light on the intricate interplay between CHDH, choline, betaine aldehyde, and betaine, and unraveled the adaptive mechanisms that *E. coli* employs in response to osmotic stress.

In summary, our work provides new insights into the structure of *E. coli* CHDH and its catalytic role in the choline metabolic pathway, as well as its role in cellular osmotic stress, and may offer implications for the functional mechanisms of eukaryotic CHDH.

4. Materials and methods

4.1. Purification of E. coli CHDH

The construct containing the CHDH gene was generated by PCR from the *E. coli* BL21 (DE3) genome, and a 6 × His tag was added at the C-terminus of *betA*. The resulting full-length PCR-amplified DNA was restricted with *Nco*I/*Hind*III, then ligated into a similarly restricted pET28a plasmid to yield pET28a-CHDH. The plasmid encoding CHDH was transformed into BL21 (DE3) cells and grown in Luria-Bertani medium containing 50 mg/ml kanamycin sulfate at 37 °C until OD600 of 0.6–0.8. The recombinant CHDH protein was expressed in the *E. coli* BL21 (DE3) strain grown at 22 °C after induction with 0.5 mM IPTG. Bacteria were collected after growing overnight (16 h) and resuspended in 50 mM KH_2PO_4 (pH 8.0), 1 mM EDTA, and 1 % complete protease inhibitor (Sigma). The suspension was passed five times through a microfluidizer (Hangzhou David Science and Education Instrument Corp.) at a pressure of 15,000 psi to disrupt the cells. The disrupted cells were centrifuged at 20,000×*g* for 20 min to remove cell debris. Membranes were obtained after centrifugation at 180,000×*g* for 4 h and stored at −80 °C. On the day of purification, the membrane pellet was resuspended in 50 mM KH_2PO_4 buffer (pH 8.0), 1 mM EDTA, and solubilized using the SMA copolymer SMA3000HNA (styrene maleic acid copolymer ca. 3:1 M ratio of styrene: maleic acid). The SMA solution was added dropwise to a final concentration of 1.0 % (wt/vol) with gentle stirring. After incubation for 2 h on ice, the solution was centrifuged at 180,000×*g* for 20 min to remove insoluble material. The solubilized fraction was loaded onto a Ni-nitriloacetic acid (NTA) (Qiagen) column pre-equilibrated with 50 mM KH_2PO_4 (PH 8.0), 1 mM EDTA. Proteins were eluted with 250 mM imidazole in the same buffer. The peak fractions from the Ni-NTA column were pooled, concentrated, and loaded onto an ENrichTM SEC 650 10 × 300 Column (Bio-Rad) equilibrated with gel filtration buffer containing 20 mM Tris-HCl (pH 7.5), 50 mM NaCl. The purest and most concentrated fractions were further concentrated using a Millipore 100 kDa cut-off concentrator and then immediately used for functional experiments and cryo-EM grid preparation. Purification using n-Dodecyl-β-D-Maltopyranoside (DDM) was performed in the same method as described above, with the exception of replacing the 1.0 % (wt/vol) SMA copolymer with 1.0 % (wt/vol) DDM to solubilize the membrane pellet and adding 0.3 % (wt/vol) DDM during all subsequent purification processes.

4.2. SDS-PAGE gel electrophoresis

Prepared a 12 % separating gel and a 5 % concentrated gel according to the instructions of the SDS-PAGE gel rapid preparation kit (Beyotime Biotechnology). The sample was diluted to the appropriate concentration to ensure that the amount of loaded protein was 20–30 μg with 20 μL of 2 × SDS loading buffer. The supernatants were then loaded and separated on a 12 % SDS-PAGE gel. The SDS-PAGE transient blue staining solution was used for staining.

4.3. His473 of CHDH mutated into Ala473

Employing appropriately designed oligonucleotide primers in overlap extension PCR, the His473 codon within pET28a-CHDH was mutated to Ala473. Subsequently, the full coding region was restricted with

*Nco*I/*Hind*III. After that, it was linked to the pET28a vector, resulting in pET28a-CHDH-H473A.

4.4. Enzymatic oxidation of choline and its derivatives

To evaluate the products generated by the reaction catalyzed by *E. coli* CHDH, the experiments were categorized into two main types: the derivatization of betaine aldehyde and the derivatization of betaine. For the betaine aldehyde derivatization, three groups were established: the standard group (betaine aldehyde), the reaction group, and a blank control group (lacking an electron acceptor). In the case of betaine derivatization, there were two primary groups: the standard group (betaine) and the reaction group, which included two distinct substrates (choline chloride and betaine aldehyde for comparison) along with their respective blank control group (also without an electron acceptor).

Derivatization reaction of betaine aldehyde [31]**:** In the standard group, the betaine aldehyde derivatization solution comprised 20 μL phenylhydrazine, 40 μL acetonitrile, and 100 μL deionized water. Then, the total volume of the mixture was 100 μL, which contained 2 μL 50 mM commercial betaine aldehyde standard, 10 μL betaine aldehyde derivatization solution, and 88 μL ddH_2O. The mixture was incubated at 37 °C for 30 min and then centrifuged at 13000×*g* for 5 min. The supernatant was directly injected into the HPLC.

In the reaction group using choline as the substrate, the total volume of the mixture was 100 μL, which contained 10 mM choline chloride, 1 mM PMS or DQ, 5 μM *E .coli* CHDH sample, and 50 mM Tris-HCl (pH 7.5). The reaction was incubated at 37 °C for 30 min, and terminated by adding 100 μL acetonitrile and 5 μL HCl. Taking 10 μL of the above mixture was added to 90 μL of the betaine aldehyde derivatization solution. After centrifugation at 13000×*g* for 5 min, the supernatant was directly injected into the HPLC. A blank control group without an electron acceptor was also established.

Derivatization reaction of betaine [32]**:** In the standard group, to prepare the betaine derivation solution, weighed 6.60 mg of 18-crown-6 and 124.50 mg of α-Bromo-2′-acetonaphthone, and dissolved them in 100 mL of acetonitrile. Next, the total volume of the mixture was 1000 μL, which contained 50 μL of 100 mM betaine standard, 50 μL of 100 mM KH_2PO_4, and 900 μL of the betaine derivatized solution. The mixture was incubated at 80 °C for 60 min and then centrifuged at 13,000×*g* for 5 min. The supernatant was directly injected into the HPLC.

In the reaction group used choline as the substrate, the total volume of the mixture was 100 μL, which contained 10 mM choline chloride, 1 mM PMS or DQ, 5 μM *E. coli* CHDH protein sample, and 50 mM Tris-HCl (pH 7.5). The mixture was incubated at 80 °C for 60 min and the reaction was quenched with 100 μL acetonitrile and 5 μL HCl. Take 10 μL of the above mixture was added to 90 μL of the betaine derivatization solution. The sample was then centrifuged at 13000×*g* for 5 min, and the supernatant was directly injected into the HPLC. A reaction control group was established, using choline chloride as the substrate as well but without an electron receptor.

The comparison group used betaine aldehyde as the substrate, the total volume of the mixture was 100 μL, which contained 5 mM betaine aldehyde, 1 mM PMS or DQ, 5 μM *E. coli* CHDH protein sample, and 50 mM Tris-HCl (pH 7.5). The mixture was incubated at 37 °C for 30 min, and the reaction was stopped by adding 100 μL acetonitrile and 5 μL HCl. Take 10 μL of the above mixture was added to 90 μL of the betaine derivatization solution. Then, the sample was centrifuged at 13000×*g* for 5 min, and the supernatant was directly injected into the HPLC. The comparison control group was set up, using betaine aldehyde as the substrate and without an electron acceptor.

All derivatization reaction results were analyzed using an HPLC system, comprising a Model 501 pump coupled to a Wisp Model 712 autosampler, a 490 Programmable Multiwavelength Detector connected to a dual channel monitor (Waters Associates), and a Shimadzu integrator CR3A. The HPLC column used was a SupelcosilTM LC-SCX, 5 μm, 25 cm*4.6 cm (Supelco Inc.). Each isocratic elution was carried out over 20 min using a mobile phase containing methanol and water. The mobile phase was degassed for 30 min in an ultrasonic bath before use. The detector reading was recorded, and all chromatography procedures were performed at room temperature.

4.5. Enzyme kinetics of CHDH

Betaine aldehyde standard curve: A standard curve for betaine aldehyde was established using a betaine aldehyde derivatization system. This system consisted of 50 mM betaine aldehyde standard or sample (2 μL), 10 μL of betaine aldehyde derivatization solution (20 μL phenylhydrazine, 40 μL acetonitrile, and 100 μL deionized water), and 88 μL deionized water. The mixture was incubated at 37 °C for 30 min and then centrifuged at 13000×*g* for 5 min. The supernatant was directly injected into the HPLC. The injection volumes were set at 0.25 μL, 0.5 μL, 1 μL, 2 μL, 5 μL, 10 μL and 15 μL for HPLC analysis. The peak areas corresponding to each injection volume were recorded. Subsequently, the peak areas were taken as the ordinate (Y), and the corresponding sample quantities were taken as the abscissa (X) to draw the standard curve for betaine aldehyde.

Enzyme kinetics in SMA3000 nanodisc: An enzyme reaction system was set up with a fixed concentration of enzyme and a concentration gradient of choline chloride, ensuring that the substrate concentration greatly exceeded the enzyme concentration (at least 100 ×). Different reaction groups included choline chloride concentrations of 0.1 mM, 0.25 mM, 0.5 mM, 1 mM, 2 mM, 5 mM, 10 mM, and 20 mM, using either 1 mM PMS or DQ as the electron acceptor. Each reaction contained 50 mM Tris-HCl (pH 7.5), 0.68 μM CHDH enzyme purified by SMA3000. The enzyme was added last and incubated for 3–5 min at 37 °C. To stop the reaction, 100 μL acetonitrile and 5 μL HCL were added. Each reaction was set up in five parallel experiments. Then HPLC analysis was carried out and the absorption peak areas were recorded. The total amount of betaine aldehyde production was calculated by the betaine aldehyde standard curve. The initial rate is expressed by the amount of product betaine aldehyde generated in unit time. Divide the total amount of betaine aldehyde by the reaction time of 3 min or 5 min to obtain a total of 40 initial reaction rates in 8 groups. The resulting initial rates and substrate concentration were fitted to the Michaelis equation to obtain K_m and V_{max}.

Enzyme kinetics in DDM nanodisc: The experimental groups, concentrations of each reaction component, and the overall process were the same as the above, with the exception of the enzyme sample. In this experiment, 1.17 μM CHDH enzyme was purified using DDM detergent, as described in the section of purification of *E. coli* CHDH above.

4.6. Electron microscopy (EM)

Negative staining EM grids preparation and data collection, processing, and model prediction [33]**:** Purified protein from gel filtration was diluted to approximately 0.008 mg/ml, and 3 μL of the sample was applied to a glow-discharged carbon-coated copper grid for 1 min. Then the grid was gently blotted with filter paper. The grid was stained with 3 % (w/v) uranyl acetate for 1 min, gently blotted again, and air-dried. Approximately 100 micrographs were collected using a Talos L120C TEM (Thermo Fisher Scientific).

Raw micrographs were processed using RELION v3.0 [34]. Structure prediction was performed by AlphaFold2 [34]. The visualization of the model was done by UCSF Chimera v 1.13.1 [35].

Cryo-EM grids preparation and data collection and processing: 3 μL of concentrated CHDH in SMA nanodisc (5 mg/ml) was added to a glow-discharged holey copper grid (Quantifoil® 300 mesh R2/3 holey carbon grid; Quantifoil Micro Tools GmbH, Germany). The grids were blotted for 2.5–4 s using a blotting force of −4 at 8 °C and 100 % humidity in a FEI Vitrobot Mark IV (ThermoFisher Scientific; Waltham, MA, USA). Grids were flash-frozen in liquid ethane and stored in liquid

nitrogen until data collection. Automatic data collection was performed on a Titan Krios microscope (Thermo Fisher), equipped with a K3 direct-electron detector (Gatan) operating at 0.832 Å per pixel in counting mode, using the SerialEM [36] software package.

Beam-induced movement of each micrograph was corrected using MotionCor2 [37] and contrast transfer function (CTF) estimation was calculated using Gctf [38]. Initial particles were picked from 1000 micrographs using autopicking and generated initial 2D class averages by RELION as the templates for automatic particle picking of the entire dataset by Gautomatch (https://www.mrc-lmb.cam.ac.uk/kzhang/).

Subsequent data processing was carried out in cryoSPARC [39] including particle extraction, 2D classification, ab-initio reconstruction, heterogeneous refinement, local refinement, and per-particle CTF refinement.

Model building: The AlphaFold predicted model of each subunit was fitted into the corresponding map as a rigid body using UCSF Chimera [35]. Figures were generated using Pymol (The PyMOL Molecular Graphics System, Schrödinger, LLC).

4.7. Osmotic stress tolerance assay

The construction of *betA* gene deletion mutant of *E. coli* C43 (C43ΔbetA) strain was performed by the gene replacement method as previously described [40], using the pKD46 plasmid. Both *E. coli* C43 wildtype cells and C43ΔbetA cells were grown at 37 °C in basic minimal M63 medium (100 mM KH_2PO_4, 75 mM KOH, 15 mM $(NH_4)_2SO_4$, 1 mM $MgSO_4$, 3.9 μM $FeSO_4$, and 22 mM D-Glucose) with no added salt until the OD600 reached 0.8 or the cells were grown to a plateau [8] and then diluted to an OD600 of 0.05 with fresh M63 medium added 600 mM NaCl. Cell growth was regularly monitored at 2-h intervals, both in the absence or presence of 1 mM choline or 1 mM betaine. After 24 h of incubation at 37 °C, the growth curves for *E. coli* C43 wildtype cells were calculated and compared to those of C43ΔbetA cells. Independent experiments were performed in triplicates.

4.8. Statistical analysis

All kinetic parameters data were obtained from at least three repeated experiments and are expressed as the Mean ± SEM (standard error of the mean). Two-group comparisons were made by the unpaired Student's t-test, and multiple comparisons were analyzed by one-way analysis of variance (ANOVA) [41]. Differences were considered significant when $p \leq 0.05$. In *vitro* data in panels represented means ± SD from three independent experiments. Quantitative analyses were carried out with GraphPad Prism 7.0 (San Diego, CA, USA).

CRediT authorship contribution statement

Xiuxiu Ma: Methodology, Data curation. **Fangling Xu:** Methodology, Formal analysis. **Koukou Yu:** Investigation. **Fan Wang:** Validation. **Quan Li:** Software. **Weifeng Liang:** Validation. **Bing Liu:** Resources. **Bo Zhang:** Conceptualization. **Jiapeng Zhu:** Writing – review & editing. **Jiao Li:** Writing – review & editing, Writing – original draft, Project administration.

Funding

This work was supported by the Young Scientists Fund of the National Natural Science Foundation of China (Grant No. 32201038 to J. L.); Nanjing University of Chinese Medicine supporting funds for the Young Scientists Fund of the National Natural Science Foundation of China (Grant No. XPT32201038 to J. L.); Key Research and Development Program of China 2020YFA0509400 (to J. P.); the Priority Academic Program Development of Jiangsu Higher Education Institutions (Integration of Chinese and Western Medicine).

Competing interests

Authors declare that they have no competing interests.

Acknowledgements

All negative staining EM data and cryo-EM data were collected at the Yale Cryo-EM Resource (YCR). We would like to thank Dr. K. Z. and S. W. for technical support on microscopy and data collection.

Abbreviations

CHDH, choline dehydrogenase; GMC, glucose-methanol-choline; DDM, N-Dodecyl-β-D-maltoside; SMA, styrene maleic acid; DQ, decylubiquinone; EM, electron microscopy; HPLC, high performance liquid chromotagraphy.

Data availability

Data will be made available on request.

References

[1] P.J. Mann, J.H. Quastel, The oxidation of choline by rat liver, Biochem. J. 31 (6) (1937) 869–878.
[2] T. Lamark, et al., DNA sequence and analysis of the bet genes encoding the osmoregulatory choline-glycine betaine pathway of Escherichia coli, Mol. Microbiol. 5 (5) (1991) 1049–1064.
[3] S. Ikuta, et al., Purification and characterization of choline oxidase from Arthrobacter globiformis, J. Biochem. 82 (6) (1977) 1741–1749.
[4] B. Landfald, A.R. Strøm, Choline-glycine betaine pathway confers a high level of osmotic tolerance in Escherichia coli, J. Bacteriol. 165 (3) (1986) 849–855.
[5] B. Kempf, E. Bremer, Uptake and synthesis of compatible solutes as microbial stress responses to high-osmolality environments, Arch. Microbiol. 170 (5) (1998) 319–330.
[6] M.B. Burg, J.D. Ferraris, Intracellular organic osmolytes: function and regulation, J. Biol. Chem. 283 (12) (2008) 7309–7313.
[7] E. Bremer, R. Krämer, Responses of microorganisms to osmotic stress, Annu. Rev. Microbiol. 73 (2019) 313–334.
[8] F. Fan, M. Ghanem, G. Gadda, Cloning, sequence analysis, and purification of choline oxidase from Arthrobacter globiformis: a bacterial enzyme involved in osmotic stress tolerance, Arch. Biochem. Biophys. 421 (1) (2004) 149–158.
[9] F. Salvi, G. Gadda, Human choline dehydrogenase: medical promises and biochemical challenges, Arch. Biochem. Biophys. 537 (2) (2013) 243–252.
[10] C.G. Figueroa-Soto, E.M. Valenzuela-Soto, Glycine betaine rather than acting only as an osmolyte also plays a role as regulator in cellular metabolism, Biochimie 147 (2018) 89–97.
[11] D.R. Cavener, GMC oxidoreductases. A newly defined family of homologous proteins with diverse catalytic activities, J. Mol. Biol. 223 (3) (1992) 811–814.
[12] T. Wongnate, P. Chaiyen, The substrate oxidation mechanism of pyranose 2-oxidase and other related enzymes in the glucose-methanol-choline superfamily, FEBS J. 280 (13) (2013) 3009–3027.
[13] L. Sützl, et al., The GMC superfamily of oxidoreductases revisited: analysis and evolution of fungal GMC oxidoreductases, Biotechnol. Biofuels 12 (2019) 118.
[14] O. Dym, D. Eisenberg, Sequence-structure analysis of FAD-containing proteins, Protein Sci. 10 (9) (2001) 1712–1728.
[15] A. Vrielink, L.F. Lloyd, D.M. Blow, Crystal structure of cholesterol oxidase from Brevibacterium sterolicum refined at 1.8 A resolution, J. Mol. Biol. 219 (3) (1991) 533–554.
[16] D.R. Haubrich, N.H. Gerber, Choline dehydrogenase. Assay, properties and inhibitors, Biochem. Pharmacol. 30 (21) (1981) 2993–3000.
[17] H. Tsuge, et al., A novel purification and some properties of rat liver mitochondrial choline dehydrogenase, Biochim. Biophys. Acta 614 (2) (1980) 274–284.
[18] A.S. Halavaty, et al., Structural and functional analysis of betaine aldehyde dehydrogenase from Staphylococcus aureus, Acta Crystallogr D Biol Crystallogr 71 (Pt 5) (2015) 1159–1175.
[19] V. Kotov, et al., High-throughput stability screening for detergent-solubilized membrane proteins, Sci. Rep. 9 (1) (2019) 10379.
[20] J.W. Patrick, et al., Allostery revealed within lipid binding events to membrane proteins, Proc. Natl. Acad. Sci. U. S. A. 115 (12) (2018) 2976–2981.
[21] P.L. Yeagle, Non-covalent binding of membrane lipids to membrane proteins, Biochim. Biophys. Acta 1838 (6) (2014) 1548–1559.
[22] M. Jamshad, et al., Surfactant-free purification of membrane proteins with intact native membrane environment, Biochem. Soc. Trans. 39 (3) (2011) 813–818.
[23] C. Logez, et al., Detergent-free isolation of functional G protein-coupled receptors into nanometric lipid particles, Biochemistry 55 (1) (2016) 38–48.
[24] S.A. Nestorow, T.R. Dafforn, V. Frasca, Biophysical characterisation of SMALPs, Biochem. Soc. Trans. 49 (5) (2021) 2037–2050.

[25] O. Quaye, et al., Role of Glu312 in binding and positioning of the substrate for the hydride transfer reaction in choline oxidase, Biochemistry 47 (1) (2008) 243–256.
[26] S. Finnegan, et al., Structural and kinetic studies on the Ser101Ala variant of choline oxidase: catalysis by compromise, Arch. Biochem. Biophys. 501 (2) (2010) 207–213.
[27] O. Quaye, S. Cowins, G. Gadda, Contribution of flavin covalent linkage with histidine 99 to the reaction catalyzed by choline oxidase, J. Biol. Chem. 284 (25) (2009) 16990–16997.
[28] O. Quaye, et al., Rescuing of the hydride transfer reaction in the Glu312Asp variant of choline oxidase by a substrate analogue, Arch. Biochem. Biophys. 499 (1–2) (2010) 1–5.
[29] F. Salvi, et al., Structure of choline oxidase in complex with the reaction product glycine betaine, Acta Crystallogr D Biol Crystallogr 70 (Pt 2) (2014) 405–413.
[30] J.J. De Ridder, K. van Dam, The efflux of betaine from rat-liver mitochondria, a possible regulating step in choline oxidation, Biochim. Biophys. Acta 291 (2) (1973) 557–563.
[31] Y. Hai, A.M. Huang, Y. Tang, Structure-guided function discovery of an NRPS-like glycine betaine reductase for choline biosynthesis in fungi, Proc. Natl. Acad. Sci. U. S. A. 116 (21) (2019) 10348–10353.
[32] M.D. Laryea, et al., Simple method for the routine determination of betaine and N, N-dimethylglycine in blood and urine, Clin. Chem. 44 (9) (1998) 1937–1941.
[33] M. Bloch, M. Santiveri, N.M.I. Taylor, Membrane protein cryo-EM: cryo-grid optimization and data collection with protein in detergent, Methods Mol. Biol. 2127 (2020) 227–244.
[34] S.H. Scheres, RELION: implementation of a Bayesian approach to cryo-EM structure determination, J. Struct. Biol. 180 (3) (2012) 519–530.
[35] E.F. Pettersen, et al., UCSF Chimera–a visualization system for exploratory research and analysis, J. Comput. Chem. 25 (13) (2004) 1605–1612.
[36] D.N. Mastronarde, Automated electron microscope tomography using robust prediction of specimen movements, J. Struct. Biol. 152 (1) (2005) 36–51.
[37] S.Q. Zheng, et al., MotionCor2: anisotropic correction of beam-induced motion for improved cryo-electron microscopy, Nat. Methods 14 (4) (2017) 331–332.
[38] K. Zhang, Gctf: real-time CTF determination and correction, J. Struct. Biol. 193 (1) (2016) 1–12.
[39] A. Punjani, et al., cryoSPARC: algorithms for rapid unsupervised cryo-EM structure determination, Nat. Methods 14 (3) (2017) 290–296.
[40] A.J. Link, D. Phillips, G.M. Church, Methods for generating precise deletions and insertions in the genome of wild-type Escherichia coli: application to open reading frame characterization, J. Bacteriol. 179 (20) (1997) 6228–6237.
[41] P. Mishra, et al., Application of student's t-test, analysis of variance, and covariance, Ann. Card Anaesth. 22 (4) (2019) 407–411.